Analysis of deep level parameters in irradiated silicon detectors

C. Betancourt *, G. Alers, N. Dawson, M. Gerling, R.F. Hurley, H.F.-W. Sadrozinski, S. Sattari

Santa Cruz Institute for Particle Physics, University of California, Santa Cruz 1156 High Street, Santa Cruz, CA 95064, United States

ARTICLE INFO

ABSTRACT

Both the collected charge and the capacitance of a silicon detector are proportional to the depleted depth of the space charge region. The presence of deep levels introduces frequency dependence in the measured capacitance, and this frequency dependence can be corrected for by analyzing the data using admittance spectroscopy. An equivalent circuit for a PN junction containing deep levels is used to accurately model deep level response. Activation energy, majority carrier cross-section and the concentration of active deep levels at the edge of the space charge region is determined. Space charge region depth as a function of the applied voltage is extracted for various detectors irradiated with neutrons and pions. When possible, depleted depths are compared to charge collection measurements.

Published by Elsevier B.V.

1. Introduction

The main operational parameter of a silicon strip detector is the bias voltage dependence of the charge collected at the electrodes, when a particle is traversing the device. We have shown before that the bias dependence of the collected charge called $CCE(V)$, and of the reciprocal capacitance from $C–V$ measurements are identical since both are dependent on the thickness of the space charge region layer [1]. This is true as long as the detector depleted from the front side near the implant. During irradiation, the bulk of some detectors go through type inversion, switching the junction to the back side. This causes charge traveling from the back to the front of the detector to get trapped before it can be received, leading to a reduction in collected charge. Unless depletion happens from the front, $C–V$ measurements and CCE measurements should not agree. Evidence of a double junction [2,3] in some devices could cause a detector to deplete from the front even in a type inverted detector, causing $C–V$ measurements and CCE to agree. Care should also be taken to correct for the frequency dependence of $C–V$ measurements by taking into account deep level response to the AC signal.

For a minimum ionizing particle (mip), the number of electron/hole pairs is generated uniformly in the detector with 73 e/μm [4], and thus the most probable charge generated is linearly proportional to the thickness of the depleted region. For this reason, the profile of the collected charge for mips, evaluated as a function of the applied reverse voltage ($CCE(V)$), should exhibit the same trend as the reciprocal of the capacitance ($1/C(V)$), since the capacitance of a parallel-plate capacitor varies inversely with its thickness. (This is important and strictly true only as long as trapping effects can be neglected, which become very important at fluences above 10^{15} neq/cm^2 [5].) Contrary to unirradiated detectors, where the doping density is a constant as a function of depth, irradiated detectors exhibit a non-uniform space charge distribution depending on the bias voltage [2,3]. The non-uniform charge distribution of deep levels arises from the filling of those deep levels by free carriers in the valence and conduction bands. The leakage current in irradiated devices is considerably larger than in unirradiated devices. One can no longer assume the concentration of free electrons and holes is negligible, and it is the spatial distribution of these free carriers that will lead to a spatial filling of deep levels, which in turn gives rise to a non-uniform charge distribution in the space charge region of the device.

It is known that irradiation alters the electrical properties of silicon by the introduction of deep levels within the band gap [6]. There have been several studies on the effects of deep levels on the capacitance and admittance of semiconductor junction devices [7–9]. As a result, the true space charge region capacitance is convoluted by the frequency response of deep levels.

This paper is presented as follows: Section 2 describes the experimental setup and data, Section 3 describes admittance measurements and their relation to the space charge depth. Section 4 presents the results. Section 5 gives a summary of the results and conclusions.

2. Experimental setup and data

Admittance measurements have been performed on silicon pad detectors produced on both p-on-n and n-on-p, FZ and MCz material. The unirradiated sensors were produced by MICRON at Sussex, UK, on 300 μm FZ wafers of about 20 kΩ cm resistivity and

MCz wafers of about $2\,k\Omega\,cm$ resistivity and by Hamamatsu Photonics (HPK) at Hamamatsu City, Japan, on $330\,\mu m$ FZ wafers of about the same resistivity. The neutron irradiation was performed at Ljubljana and pion irradiation was performed at PSI in Switzerland.

The charge collection and C–V measurements on microstrip detectors have been performed at SCIPP, UC Santa Cruz. The $CCE(V)$ investigations have been carried out with a ^{90}Sr beta source, described in Ref. [10]. $CCE(V)$ measurements were taken up to 1100 V. The admittance experimental setup is based on a HP 4284A LCR meter coupled with the HP 16065A text fixture (modified to permit biasing with voltages up to 700 V). Voltage sourcing and current monitoring are performed through a computer-controlled Keithley 2410 HV supply. In order to reduce the leakage current noise, $CCE(V)$ are taken at $-20\,°C$. More details on the experimental system for $CCE(V)$ are given in Ref. [1].

The temperature was varied in between admittance measurements, ranging from 0 to 20 °C in 5 °C steps. During each measurement, the temperature was kept constant using a cooling setup that included peltiers for cooling, and liquid nitrogen gas boil off to remove moisture from the air; so no ice forms on the detectors. Several frequencies, ranging from 100 Hz to 2 MHz, of the AC signal imposed by the LCR meter were cycled through at the beginning of each new voltage run. Admittance measurements were taken only up to 630 V and for detectors that did not deplete before this, the depletion voltage was taken from previous data on the corresponding detectors. Simulations were produced assuming two dominant deep levels, although one deep level was clearly more dominant than the other.

3. Admittance measurements and the space charge region

There are four competing processes that are involved in generation/recombination through a deep level: emission of an electron into the conduction band, capture of an electron from the conduction band, emission of a hole into the valence band and capture of a hole from the valence band. These four processes determine the steady-state filling and charge state of deep levels. When an AC signal is applied to the device, deep levels respond to the signal by filling and emptying through generation /recombination. The response of the deep levels depends on the frequency used. Each deep level will respond to the AC signal independent of the other deep levels. The frequency, in which the deep levels start to contribute to the capacitance, is the frequency that corresponds to the emission rate of that level. Since the minority free carrier density is much less than the majority free carrier density, we can neglect minority carrier response to the AC signal in the bulk. The relaxation time associated with this level for n-type material is given by [7,8]

$$\tau_t = (2e_{n,t})^{-1} \tag{1}$$

and for p-type by

$$\tau_t = (2e_{p,t})^{-1} \tag{2}$$

where $e_{n,t}$ and $e_{p,t}$ are the emission rates for electrons and holes, respectively.

The frequency response of the deep levels can more easily be studied by looking at the complex admittance of a device:

$$Y = Z^{-1} = G_p + j\omega C_p \tag{3}$$

where the capacitor and resistor in series of the impedance is turned into a capacitor and conductor in parallel. In order to model the contribution to the conductance and capacitance, an equivalent circuit model taking into account the contribution of generation–recombination and crossover capacitance to the admittance must be used. An equivalent circuit for a junction containing deep levels is derived in both Refs. [7,8], and displayed in Fig. 1. In this model, G_p/ω is given by

$$G_p/\omega = \sum_{traps} C_{bt} \frac{\ln(1 + \omega^2 \tau_t^2)}{2\omega\tau_t} \tag{4}$$

and C_p is given by

$$C_p = C_{hf} + \sum_{traps} C_{bt} \frac{\tan^{-1}(\omega\tau_t)}{\omega\tau_t} \tag{5}$$

Here C_{bt} is the capacitance of the number of active bulk deep levels within a few kT of the crossover with the bulk Fermi level and is given by [7]

$$C_{bt}(V) = \frac{\sqrt{2}C_d(V)N_t}{N_{t-1}}(1 - E_t/E_f)^{-1/2} \tag{6}$$

where $C_d(V)$ is the space charge region capacitance, N_t is the number of active concentration of the tth deep level, and N_0 is the original doping of the device. For low to moderate fluences ($<10^{15}$ neq) the term $(1-E_t/E_f)^{-1/2}$ is taken to be close to unity and the term N_{t-1} is taken to be the original doping concentration N_0. The term C_{hf} is the high-frequency capacitance and is given by [8,9]

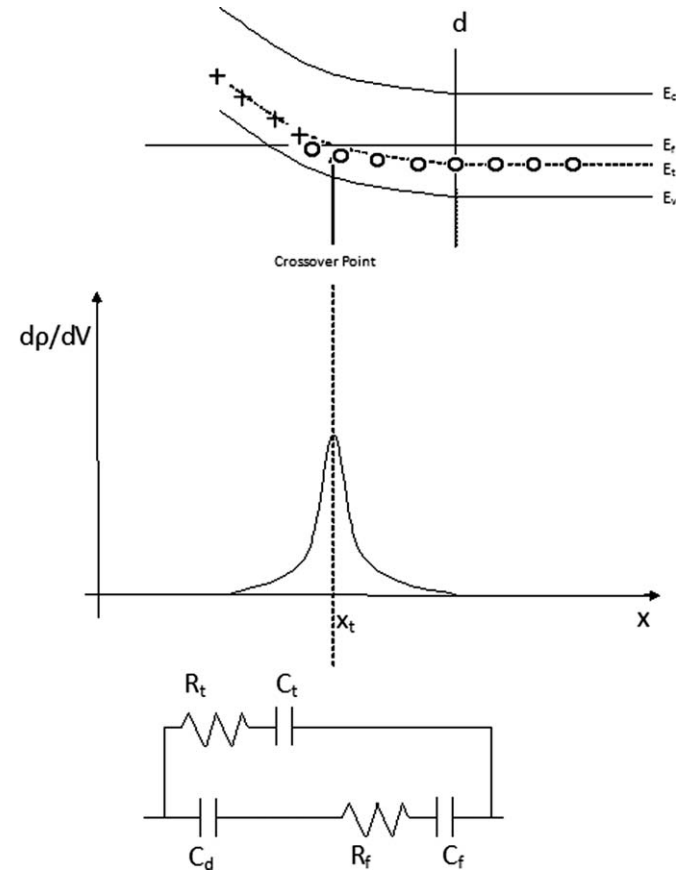$$C_{hf} = (1/C_d + 1/C_f)^{-1} \tag{7}$$

Fig. 1. Energy band diagram for a junction containing deep level, with the corresponding equivalent circuit. The generation/recombination contribution to the admittance of each deep level can be modeled as a capacitor and resistor in series.

where C_f is the flatband capacitance associated with the free carrier concentration at the edge of the space charge region. For increasing fluences, C_f dominates the high-frequency capacitance and as a result C_{hf} becomes less and less voltage dependent with increasing deep level concentration [9].

We take the capacitance of the space charge region at depletion to be given by

$$C_d(V_{dep}) = \varepsilon A/(W - L_D) \qquad (8)$$

where W is the total width of the device and L_D is the Debey length associated with C_f. Combining Eqs. (6) and (8) results in

$$d(V) = \frac{C_{bt}(V_{dep})}{C_{bt}(V)}(W - L_d) \qquad (9)$$

which gives the depth of the space charge region in an irradiated silicon detector.

4. Extraction of deep level parameters

Now that the effect of deep level response to the admittance is known, the energy, majority capture cross-section and concentration of active deep levels within a few kT of the Fermi level can be determined. From Eq. (4) a maximum in G/ω curve is observed whenever

$$\omega_p \tau_t = 1.98 \qquad (10)$$

where ω_p is the value of the angular frequency where the maximum occurs. From this and Eqs. (1) and (2) the temperature dependence of the peak frequency is determined by

$$\omega_p = 2(1.98)c_{n,p}N_{c,v}e^{\mp(E_{c,v}-E_t)/kT} \propto T^2 e^{\mp(E_{c,v}-E_t)/kT} \qquad (11)$$

where $c_{n,p}$ are the capture probabilities for electrons and holes, $N_{c,v}$ is the density of states in the conduction and valence bands, and $E_{c,v}$ are the energy of the band edges. An Arrhenius plot can then be used to determine E_t (as seen in Fig. 2) by varying the temperature and recording where the peak in G/ω is observed. The peak of the G/ω curve can easily be seen in Fig. 3, which displays the measured and the simulated admittance curves as functions of frequency. Once the activation energy of the deep level is known, the majority capture cross-section can easily be calculated from Eq. (11). The capacitance of the depleted region C_d is determined from Eq. (8), once the capacitance of the deep level as a function of voltage and the flatband capacitance is known. The flatband capacitance is taken to be the high-frequency
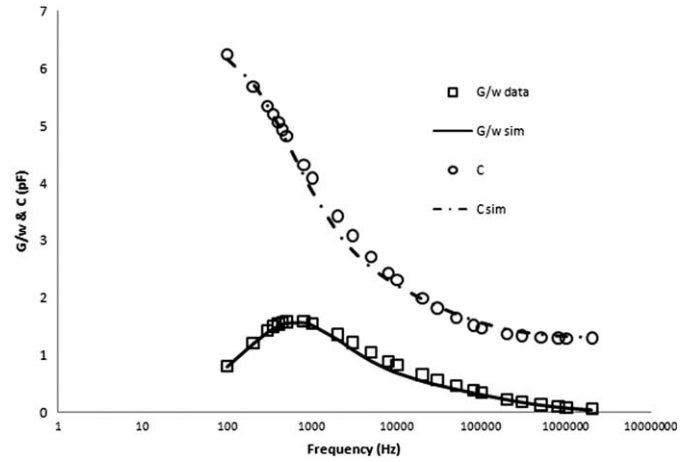

Fig. 2. Arrhenius plot for pion-irradiated p–n FZ detector.

Fig. 3. Measured and simulated C and G/ω as a function of frequency for a pion-irradiated n-type FZ detector taken at 100 V and 22 °C.
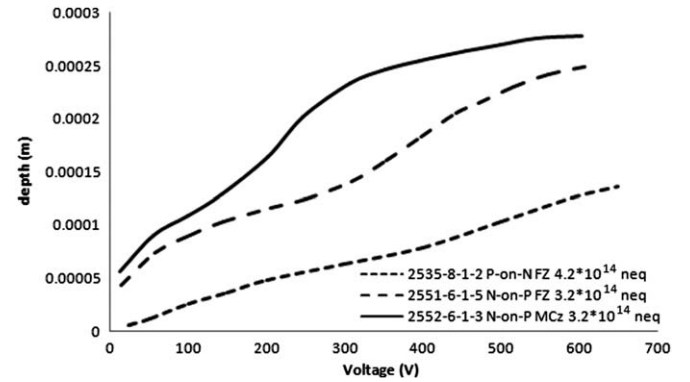

Fig. 4. Depleted depth of the space chare region for various pion detectors calculated using Eq. (9).

capacitance for moderate to highly irradiated sensors. For low fluences, C_d will dominate the high-frequency capacitance, and hence C_d can be taken to be the high-frequency capacitance. The concentration of active deep levels within a few kT of the crossover point can be determined once C_d and the original doping concentration are known, and then by plugging them with Eq. (6).

5. Results and discussion

The depth of the space charge region for several detectors of different types, irradiations, and fluences was calculated using Eq. (9). Depleted depths of the space charge region are displayed in Fig. 4 for various pions irradiated and Fig. 5 displays these for various neutron-irradiated detectors. Charge collection measurements are compared to the depleted depth for one p-on-n FZ pion, (see Fig. 6), and one n-on-p MCz neutron, (Fig. 7), irradiated detector and good agreement is observed.

Deep level parameters for the most dominant deep level were extracted and presented in Table 1. Energy level, majority carrier capture cross-section, active concentration at the crossover, and average concentration from the depletion voltage are presented. All energies are taken with respect to the conduction band.

The energy of the deep level is close to midgap as expected. The concentration of active deep levels at the depletion edge (N_t) is larger for pion than for neutron detectors, although the average
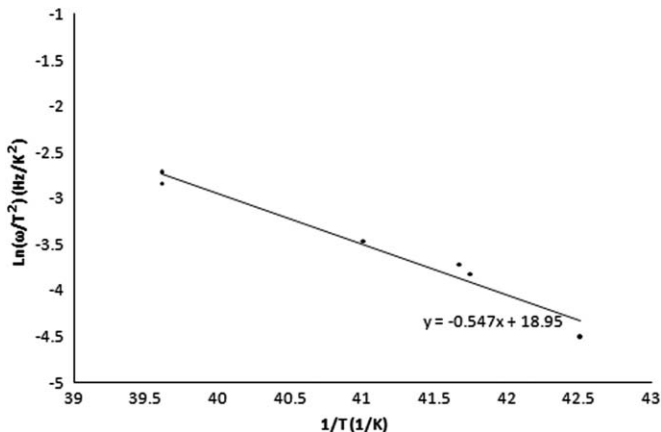
density (taken from V_{dep}) seems to be higher for neutrons. Capture cross-sections are larger for neutrons than for pions.

Although the method described in this paper gives a good idea of the concentration of deep levels, it is not sensitive to the charge
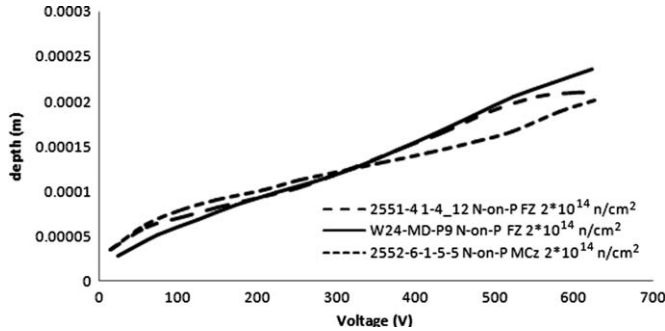

Fig. 5. Depleted depth of the space charge region for various neutron detectors calculated using Eq. (9).
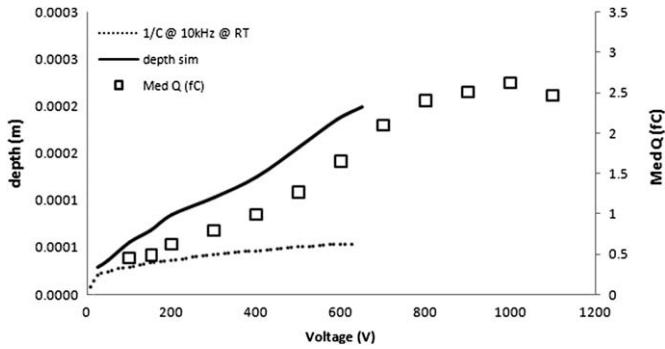

Fig. 6. Extracted depth of the space charge region compared to charge collection for p-on-n FZ pion-irradiated sensors.
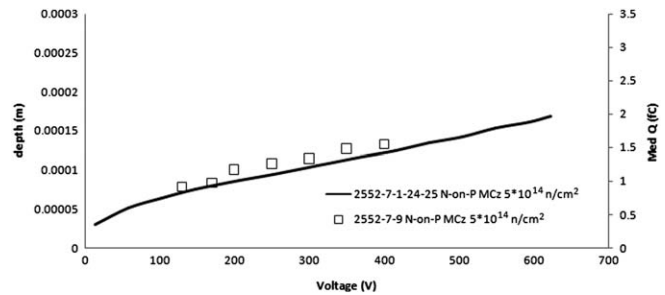

Fig. 7. Extracted depth of the space charge region compared to charge collection for n-on-p MCz neutron irradiated sensors.

of the deep levels. This means that type of deep level, donor or acceptor, cannot be known by this method alone, and must be inferred by other measurements. One possibility is to look for inversion from CCE measurements, and then determine that the dominant deep level must be the type opposite to the original if inversion occurs.

This method is also insensitive to the presence of a double junction that may arise in irradiated devices [2,3]. Only one junction is assumed in the analysis above, but this method can still be of use in a double-junction model. Although this method cannot determine the presence of a double junction, capacitance $C_d(V)$ is the capacitance across the entire space charge region, which includes both junctions if a double junction exists. This means that the total depleted depth $d(V)$ is the sum of depths of both junctions in the case of a double junction. This is due to the fact that free charge carriers are sampling the entire device when they fill and empty the deep levels.

Since good agreement is observed when the space charge depth determined from Eq. (9) is compared to the collected charge of a corresponding detector, this indicates that both sensors are depleting from the front side. If any of these have gone through type inversion, it could imply the presence of a double junction [2,3]. The good agreement between the corrected depth and charge collection also shows that the corrected C–V measurements are a good indicator of the collected charge as a function of voltage for detectors as long as inversion does not occur. This could eliminate the need to measure collected charge in many cases, and instead perform a much simpler C–V measurement in its place.

6. Conclusions and summary

We have shown that by studying the admittance of an irradiated device, important information is revealed about the most dominant deep levels introduced by irradiation. The frequency response of the deep level can be determined by constructing an equivalent circuit that takes into account generation and recombination through deep levels as well as any effect that free carriers have on the device. The equivalent circuit provides the connection between the measured admittance and steady-state filling and emptying of deep levels inside our device.

Once the admittance is modeled using Eqs. (4) and (5), deep level parameters can be extracted from fitting the model to the data. The amplitude of the peak in the G/ω is directly proportional to both the depletion capacitance and the number of active deep levels within a few kT of the Fermi level. So once C_d is known, N_t can be calculated using Eq. (6). The energy E_t of the deep level can be determined from the temperature dependence of the peak frequency ω_p by taking the slope of the Arrhenius plot. Once the energy is known, it can be plugged into Eq. (11) along with ω_p to determine the majority carrier capture cross-section.

Table 1
Deep level parameters.

Pion detector	Fluence	N_{act} (1/cm^3)	N_{eff} (1/cm^3)	E_t (eV)	Capture cross (cm^2)
n-on-p MCz	3.2×10^{14}	1.67×10^{13}	7.19×10^{12}	−0.544	7.7×10^{-15}
n-on-p FZ	3.2×10^{14}	2.73×10^{12}	7.91×10^{12}	−0.55	9.8×10^{-15}
p-on-n FZ	4.2×10^{14}	3.53×10^{12}	9.35×10^{12}	−0.547	8.7×10^{-15}
Neut. detector					
n-on-p MCz	5×10^{14}	7.17×10^{12}	1.09×10^{13}	−0.56	2.35×10^{-14}
n-on-p FZ p-spray	2×10^{14}	8.00×10^{11}	5.76×10^{12}	−0.576	4.40×10^{-14}
p-on-n FZ	2×10^{14}	1×10^{12}	5.76×10^{12}	−0.575	4.20×10^{-14}

References

[1] M.K. Petterson, et al., RRESMDD06, Nucl. Instr. and Meth. A (2007), doi:10.1016/j.nima.2007.08.222.

[2] V. Chiochia, et al., Simulation of heavily irradiated pixel sensors and comparison with test beam measurements. IEEE Nucl. Sci. Symp., October 20.

[3] V. Eremin, E. Verbitskaya, Z. Li, Nucl. Instr. and Meth. A 476 (2002) 556.

[4] W.M. Yao, et al., J. Phys. G: Nucl. Part. Phys. 33 (2006) 265 (Chapter 27).

[5] G. Casse, P.P. Allport, S. Martí i Garcia, M. Lozano, P.R. Turner, Nucl. Instr. and Meth. A 518 (2004) 340.

[6] M. Bruzzi, et al., Nucl. Instr. and Meth. A 552 (2005) 20.

[7] E.H. Nicollian, J.R. Brews, MOS (Metal Oxide Semiconductor) Physics and Technology, 2003 (Hoboken, NJ: John Wiley & Sons, Inc.) ch 4,5.

[8] M. Beguwala, C.R. Crowell, Solid-State Electron. 1 (7) (1974) 203.

[9] M.P. Verkhovodov, H.P. Peka, D.A. Pulemyotov, Semicond. Sci. Technol. 8 (1993) 1842.

[10] M.K. Petterson, et al., Determination of the charge collection efficiency in neutron irradiated silicon detectors, SCIPP Preprints SCIPP 08/09.